



Seismic performance and retrofit of precast concrete grouted sleeve connections

Andrea Belleri and Paolo Riva

Precast concrete structures are used worldwide because of their shorter construction time, cost effectiveness, and better plant control of structural elements and materials compared with cast-in-place concrete structures.

In Italy, the most common applications of precast concrete buildings are industrial warehouses and commercial malls. The typical structural layout of these buildings consists of cantilever columns connected by simply supported precast, prestressed concrete beams that support prestressed concrete roof elements. The columns are inserted and grouted in place in isolated precast concrete socket foundations.

This structural layout reduces construction time and is cost effective. However, this effectiveness could be compromised for construction in seismic regions, especially if the design follows the capacity design rule. The design of column footings is based on the assumption that a plastic hinge may develop at the column base in an earthquake event, while capacity design is used to prevent the formation of an inelastic mechanism in the footing. The latter goal is achieved by considering the bending moment associated with the column base flexural capacity acting on the foundation amplified by an overstrength factor. Following this design approach, the foundation base becomes large,

- Experimental tests on the cyclic behavior of column-to-foundation subassemblies were conducted to compare the response of grouted sleeve connections with those of cast-in-place and pocket-foundation connections.
- Confinement by the grouted sleeves inhibited buckling of the longitudinal reinforcement and increased the compressive strength of the grout.
- The damage was localized to the column base, allowing easier postseismic column repair compared with traditional connections.

even for medium-sized columns. This could limit the cost effectiveness of industrial and commercial precast concrete structures. In fact, because of the foundation's dimension, the footings must be cast-in-place concrete, making the use of isolated socket foundations less attractive.

Hence, mat foundations are more convenient than isolated footings. When using mat foundations, the following column-to-foundation connections are typically used:¹⁻³

- bolted base plates embedded in the foundation
- foundation pockets in which the columns are placed and grouted
- grouted sleeves
- mechanical splices

This paper investigates the behavior and performance of grouted corrugated steel sleeve connections under cyclic loading. While the behavior of precast concrete socket base connections is well documented,⁴⁻⁶ no published experimental results concerning the cyclic response of grouted sleeve column-to-foundation connections have been found.

Although temporary bracing is needed for erection stability, grouted steel sleeves are an inexpensive type of connection, especially if the retrofit after a seismic event is considered. The confinement provided by grouted steel sleeves inhibits buckling of the longitudinal reinforcement and increases the strength of the grout. As a result, the damage associated with this kind of connection is localized to the column base, allowing easier postseismic column repair compared with traditional connections.

Another advantage of grouted steel sleeve connections compared with modern mechanical splice devices is the ability to include an unbonded portion in the reinforcing bar inside the sleeves. This distributes the reinforcing bar deformation over the unbonded length, increasing the ultimate rotation capacity of the subassembly and reducing the reinforcement strain demand for a given column drift (defined as the interstory displacement divided by the interstory height). This advantage is not typical of mechanical splice devices. The unbonded length of the reinforcement can be taken into account in the design process by considering an appropriate plastic hinge length.

The responses of five columns subjected to a cyclic top horizontal displacement history were investigated considering different connection details.

The cyclic behavior of a grouted corrugated steel sleeve connection with partly unbonded bars in the sleeves was investigated and compared with the cyclic behavior of the same specimen after retrofitting.

Experimental program

Test setup

This experimental program included six tests: one on each of five specimens with different column-to-foundation connections and approximately the same maximum bending moment capacity and a test on one of the original specimens after retrofitting. The columns had cross sections of 400 mm × 400 mm (16 in. × 16 in.) and heights of 3200 mm (126 in.). Two hollow-core plunger jacks applied a constant axial force of 600 kN (140 kip) to all columns. The axial force represents a gravity load compatible with the structural framing system. An electromechanical screw jack with a 500 mm (20 in.) maximum stroke and 1000 kN (225 kip) capacity applied a cyclic horizontal displacement at the top of the column, imposing an increasing column drift from 0.25% to 5%. **Figure 1** shows the test setup.

The horizontal loads and displacements were recorded by a load cell and a string pot transducer, respectively, while three pairs of linear displacement transducers evaluated the average column curvature recorded at three consecutive levels of the column base (**Fig. 2**). The lower pair of displacement transducers was connected directly to the foundation. Therefore, the average curvature evaluated comprises the strain penetration of the reinforcing bars into the foundation block.

Figure 3 shows the geometry of the tested specimens. Specimen CP represented a typical cast-in-place concrete column-to-foundation connection, and specimen PF represented a typical grouted pocket foundation with no extra roughening of the surfaces at the column and foundation interface. Specimens GS4 and GS4B both had four grouted sleeves, but each specimen had a different anchorage length of the reinforcing bars in the foundation. The specimen GS4 had 90° hooks at the reinforcing bar ends, whereas GS4B had straight reinforcing bars, which represented a connection sometimes adopted to increase construction speed. Specimen GS4U was equal to specimen GS4B with an additional 300 mm (12 in.) unbonded length on the spliced reinforcing bars. Adhesive tape provided the unbonding for these bars. GS4UR was specimen GS4U after retrofitting. The retrofitting sequence consisted of clearing the grout crushed during the previous tests at the column base, placing collar formwork, and filling it with high-strength shrinkage-compensating grout.

Material properties

All reinforcing steel had a specified yield stress greater than 450 MPa (65 ksi), but an average yield stress of 530 MPa (77 ksi) was recorded. The concrete type was C35/45 (that is, with a specified 28-day cylindrical and cubic compressive strength greater than 35 MPa [5.1 ksi] and 45 MPa [6.6 ksi], respectively). All of the grout that was

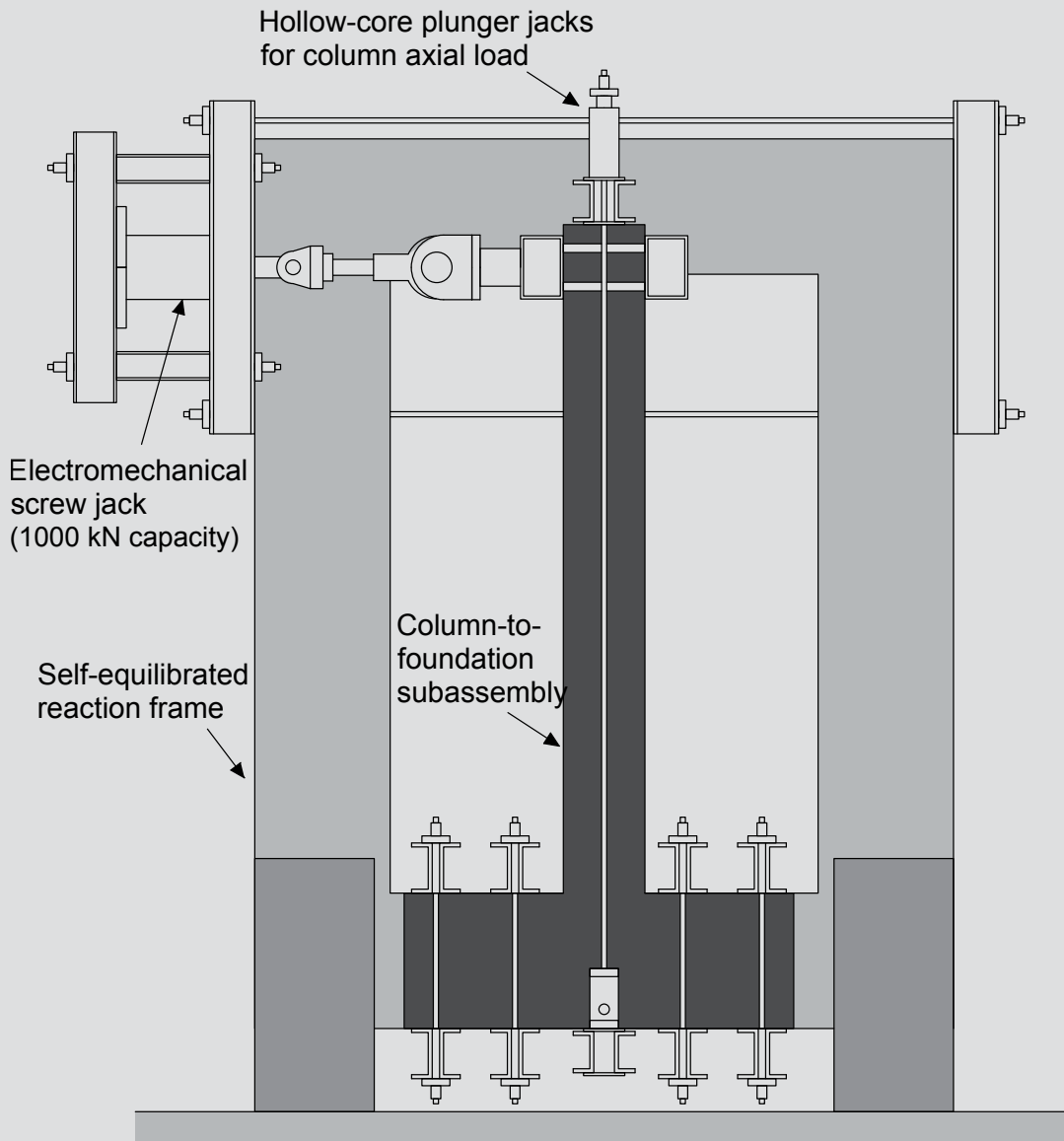


Figure 1. Test setup. Note: 1 kN = 0.225 kip.

used inside the sleeves, retrofitted connection for GS4UR, and pocket foundation PF was a shrinkage-compensating cement-based grout with a maximum aggregate size of 2.5 mm (0.1 in.) and a specified 28-day strength greater than 75 MPa (11 ksi). The ducts used for the grouted sleeve connections were typical post-tensioning ducts made with corrugated galvanized strip steel with an 80 mm (3 in.) internal diameter, an 84 mm (3.3 in.) external diameter, and a 0.6 mm (24-gauge) thickness.

Test results

Figure 4 shows the experimental horizontal load versus drift curves for the tested specimens. The lateral load was reported as measured by the load cell with no correction

for the 2nd order load-displacement effects $P-\Delta$, indicated by the dashed lines. Any gain or loss of strength is obtained when the experimental curve in absolute terms lies above or below the $P-\Delta$ lines, respectively. **Figure 5** shows the horizontal load versus drift comparison between the unbonded grouted sleeve connection before and after retrofitting.

Figure 6 shows pictures of the damaged region at the base column corresponding to 5% drift for all tests except GS4UR, which failed at approximately 3.5% drift.

The three pairs of linear displacement transducers at the column base side computed the column average curvature at three consecutive levels (low, intermediate, and high) at

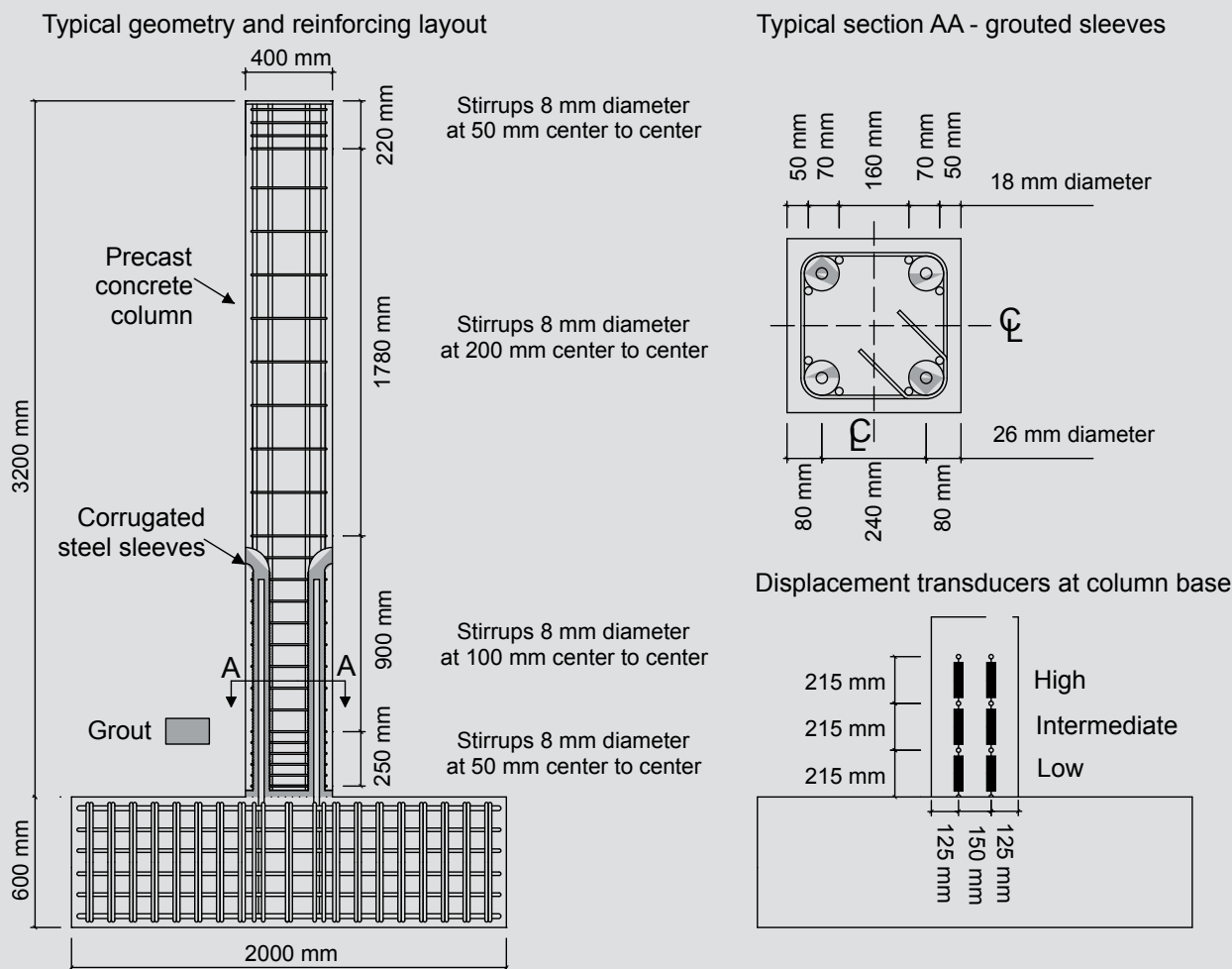


Figure 2. Reinforcement layout and instrumentation details. Note: 1 mm = 0.0394 in.

215 mm (8.46 in.) spacing. For each level, the average curvature was computed by dividing the difference between the measurements of the two displacement transducers by the level spacing (215 mm) and by the distance between the transducers (150 mm [5.9 in.]). The curvature computed at the lowest level comprises the strain penetration of the reinforcing bars into the foundation block because the displacement transducers were connected directly to the foundation. The moment-curvature curves (Fig. 7) are the envelope curves for each test, computed as the average of both directions of excitation. The abscissa is made dimensionless by multiplying the curvature by the column cross-section height B (400 mm [16 in.]).

Figure 8 shows the dimensionless energy for each test in the drift range from 1% to 5%. The dimensionless energy is defined as the ratio between the hysteretic energy (area inside each complete force-displacement cycle) and the corresponding elastic energy in a semicycle (defined as one half of the maximum displacement times the corresponding lateral force), which accounts for the equivalent horizontal

load due to the $P-\Delta$ effect.

Analysis of results

As expected, all of the columns had almost the same maximum lateral force capacity, though some differences arose due to misalignment of the reinforcing bars during construction.

The cast-in-place concrete column specimen CP failed at 5% drift due to the tensile failure of one of the reinforcing bars. This is likely due to low-cycle fatigue of the bar and localized strain at the column base where a major crack opened (Fig. 6). The column cyclic behavior was stable up to 2.5% drift, and no damage other than base concrete spalling was observed. Significant pinching was present in the cycles after 2.5% drift.

The grouted pocket foundation specimen PF showed a stable response though a small amount of strength degradation was registered in one loading direction after 3% drift.

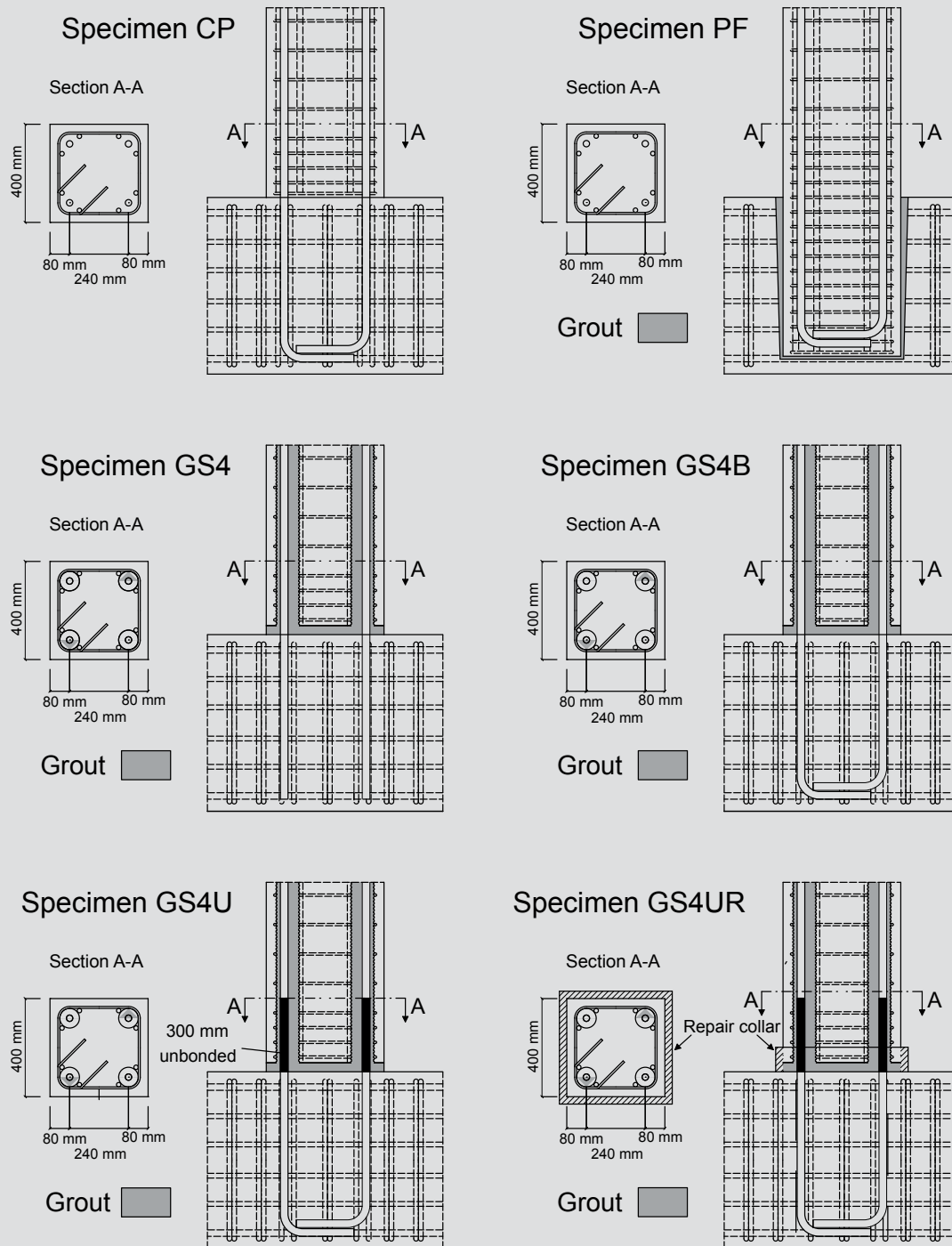


Figure 3. Details of column-to-foundation connections. Note: 1 mm = 0.0394 in.

In the same loading direction fatter hysteresis half loops were observed compared with the other loading direction. This asymmetry was probably due to imperfect centering of the column in the pocket foundation. Compared with others, specimen PF showed a more pronounced extension of flexural cracks at the column base (Fig. 6), spreading along a length approximately equal to the column base

dimension.

Specimens GS4 and GS4B showed a stable hysteretic response, though specimen GS4 showed some strength degradation starting at 2% drift. This was likely due to longitudinal reinforcement slippage in the foundation block. Specimen GS4 resembled a connection sometimes

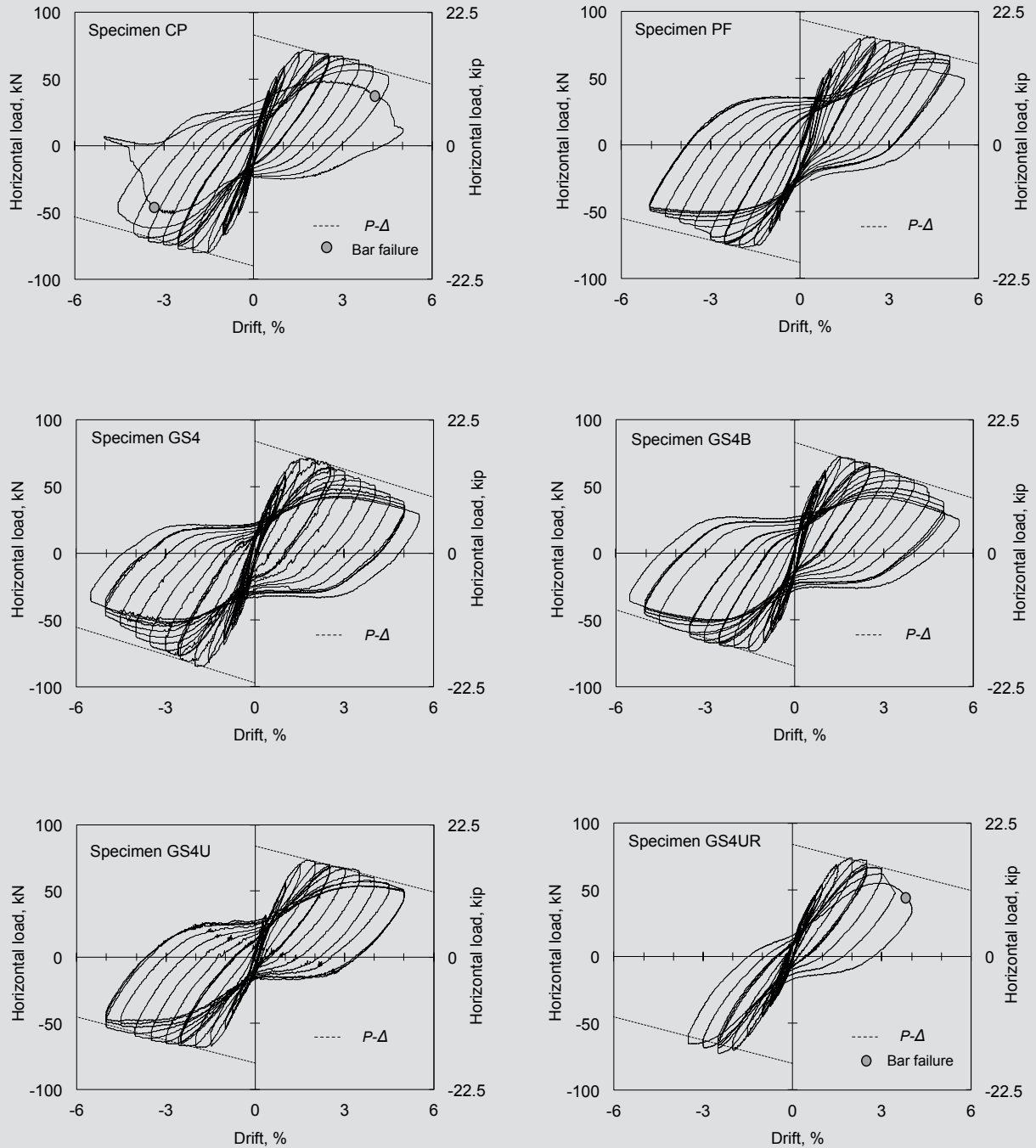


Figure 4. Lateral load versus column drift for the different connection types. Note: $P-\Delta$ = 2nd order load-displacement effects.

adopted in practice to increase construction speed even if full anchorage strength of the splice reinforcement is not provided. As expected, the limited anchorage length resulted in strength degradation in the cyclic response. This degradation is negligible for drift values smaller than 2.5%,

a value over which considerable damage is expected in nonstructural members, such as cladding panels.

The use of grouted steel sleeves on the column induced a major crack opening at the grout layer beneath the sleeves. The compressive strain concentration at the column base led to progressive damage at the unconfined grout next to

the steel sleeves. After crushing, the damaged grout was expelled from the column base, leaving the role of resisting compressive forces associated with cyclic bending to only the confined grout in the steel sleeves and the vertical reinforcing bars. On the other end, grouted steel sleeve specimens showed no other noticeable sign of damage.

Compared with traditional connections (specimens CP and PF), a slightly more pronounced pinching was observed in the cycles of GS4 and GS4B. This was due to the progressive damage of the base grout layer, which led to a larger strain localization at the column base. For these specimens, the test was extended to 6.5% drift with no reinforcing bar failure. The higher displacement capacity recorded was due to the confinement induced by the steel sleeves on the grout.

Although the localized strain at the base of specimens GS4 and GS4B could lead to a failure of the columns, the existence of confined grout regions within the sleeves effectively prevented an early failure of the connections. Furthermore, the grouted sleeves prevented buckling of the vertical bars anchored in the foundation.

Because the damage was limited to the grout layer existing at the base and the remaining part of the column was mostly undamaged, it is concluded that the grouted steel sleeve connections are easier to repair after a seismic event than the traditional connections (specimens CP and PF).

The same observations and considerations made for specimens GS4 and GS4B apply to specimen GS4U. The addition of an unbonded length in the reinforcement inside the grouted steel sleeves further reduced the column damage. The constant strain distribution in the unbonded region led to a rigid rotation at the column base, which reduced the reinforcing bar strain required to reach the same column top displacement compared with specimens GS4 and GS4B.

After reaching 5% drift, specimen GS4U was retrofitted and became specimen GS4UR. Figure 5 compares specimen GS4U with its retrofitted connection specimen GS4UR. The cyclic response of the two specimens is similar up to 3% drift. At 3.5% drift, a bar failed in specimen GS4UR. This failure was likely due to low cycle fatigue of the reinforcing bar, considering the number of cycles experienced by the specimen during both tests.

From the moment-curvature envelope curves for each test (Fig. 7), the following observations were made:

- In the high level (Fig. 2), all of the specimens behaved as linear elastic.
- In the intermediate level, specimen PF was the only specimen to behave inelastically; this is in accordance with the crack pattern in Fig. 6.

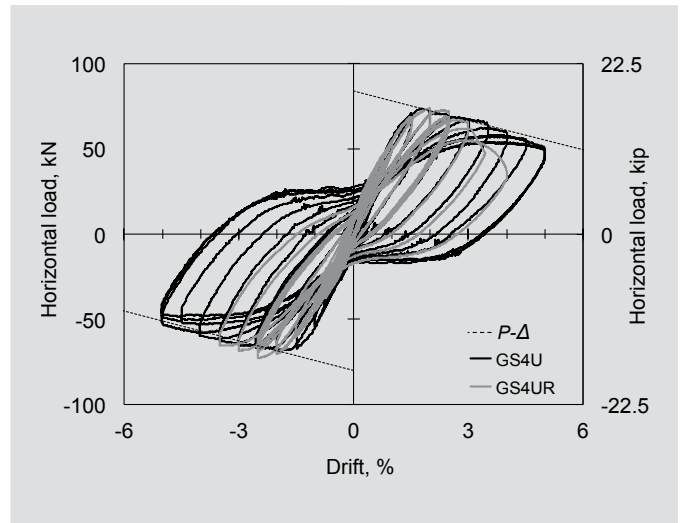


Figure 5. Comparison of lateral load–column drift between unbonded and retrofitted grouted sleeve solution. Note: $P-\Delta$ = 2nd order load displacement.

- For all of the tests, the majority of the curvature demand was concentrated at the column base as expected. The average curvature computed in the low level comprises the strain penetration of the reinforcing bars into the foundation. In fact, the displacement transducers were connected directly to the foundation block.
- The curvature of specimen CP showed a greater localization with respect to that of specimen PF; this led to the early bar failure observed in specimen CP.
- The curvature values were consistently higher for all of the grouted sleeve specimens than for the cast-in-place and pocket foundation connections. This effect once more demonstrates that a larger localized strain occurred in the grouted sleeve specimens than in the cast-in-place and pocket foundation specimens.
- Among grouted steel sleeve connections, specimen GS4 had higher curvature values than GS4B because of bar slippage.
- The unbonded connection of specimen GS4U showed the highest curvature values due to the elongation associated with the constant strain distribution in the unbonded region.

Regarding the energy dissipation for each test in the drift range of 1% to 5% (Fig. 8), no significant differences were recorded among specimens CP, PF, GS4, and GS4B, while specimens GS4U and GS4UR showed less energy dissipation because of the rotation at the column base associated with the constant strain in the unbonded region.

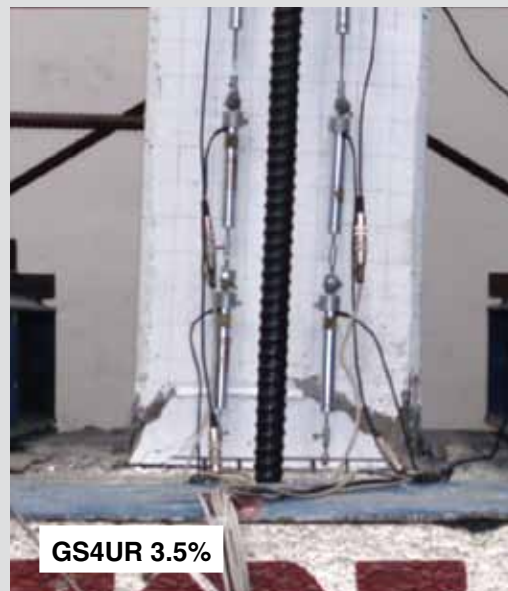
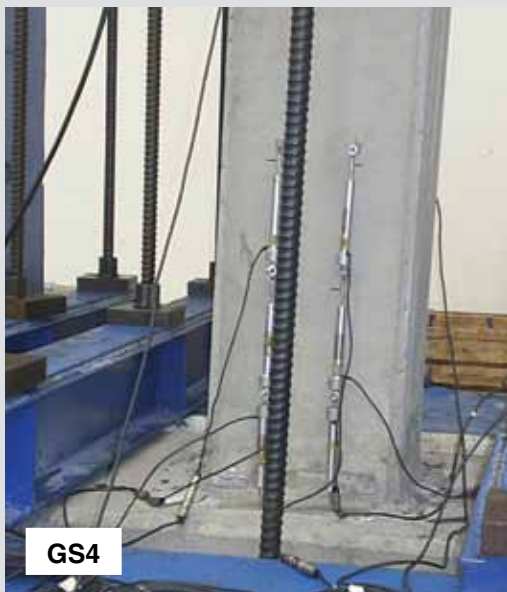


Figure 6. Damage at 5% lateral drift. Specimen GS4U was repaired and renamed GS4UR; the latter experienced the failure of one reinforcing bar at a drift of 3.5%.

Considerations on the unbonded length

As shown by the experimental results, providing an unbonded length in the longitudinal reinforcement inside the grouted steel sleeves led to a better seismic performance of the column-to-foundation connection compared with traditional connections. The longitudinal reinforcement buckling is inhibited by the confinement provided by the grouted steel sleeves, and the use of an unbonded length of reinforcement leads to an increase in the column displacement capacity. Furthermore, the damage caused by the superimposed cyclic displacement history is limited to the grout layer existing at the base, allowing easier connection repair after a seismic event compared with the other connections analyzed.

Having proved the effectiveness of the unbonded length, the next step is to determine how to take it into account in the design process and how to evaluate the column curvature ϕ and the curvature ductility μ_ϕ for different degrees of lateral displacement. The value of μ_ϕ can be directly implemented in some design procedures based on displacement control.⁷⁻⁹

To take the unbonded length into account, it is sufficient to add its value to the plastic hinge length L_p , that is, the length over which strain and plastic curvature are considered constant and equal to the maximum values at the column base, according to a bilinear idealization of the curvature distribution (Fig. 9). The new plastic hinge length, which accounts for debonding, is calculated by adding the unbonded length L_{unb} to a plastic hinge formulation provided by Priestley et al.,⁹ leading to Eq. (1).

$$L_p = 0.2 \left(\frac{f_u}{f_y} - 1 \right) L_c + L_{sp} + L_{unb} \geq 2L_{sp} + L_{unb} \quad (1)$$

where

f_u = steel ultimate stress

f_y = steel yield stress

L_c = column contraflexure length, corresponding in this case to the column height H

L_{sp} = strain penetration length, which takes into account the splice reinforcement tension strain distribution into the foundation⁹

= $0.15 f_y d_b$ if f_y is in ksi

= $0.022 f_y d_b$ if f_y is in MPa

where

d_b = reinforcing bar diameter

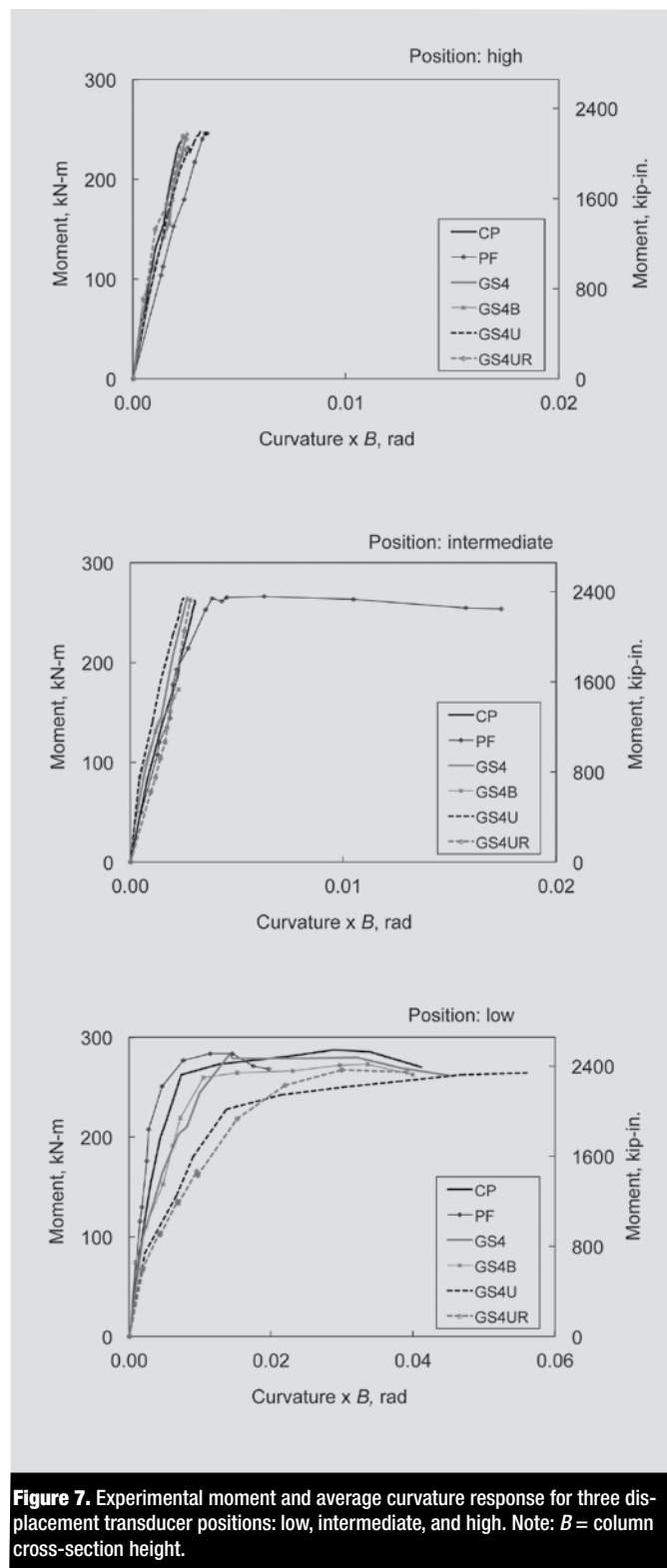


Figure 7. Experimental moment and average curvature response for three displacement transducer positions: low, intermediate, and high. Note: B = column cross-section height.

The approximations of the yield Δ_y and ultimate Δ_u column displacements are obtained by double integration of the idealized curvature distribution. In Δ_y evaluation, the rotation associated with the constant strain distribution in the unbonded region needs to be added. In the case of Δ_u , this rotation is taken into account directly by the plastic hinge length calculation proposed in Eq. (1).

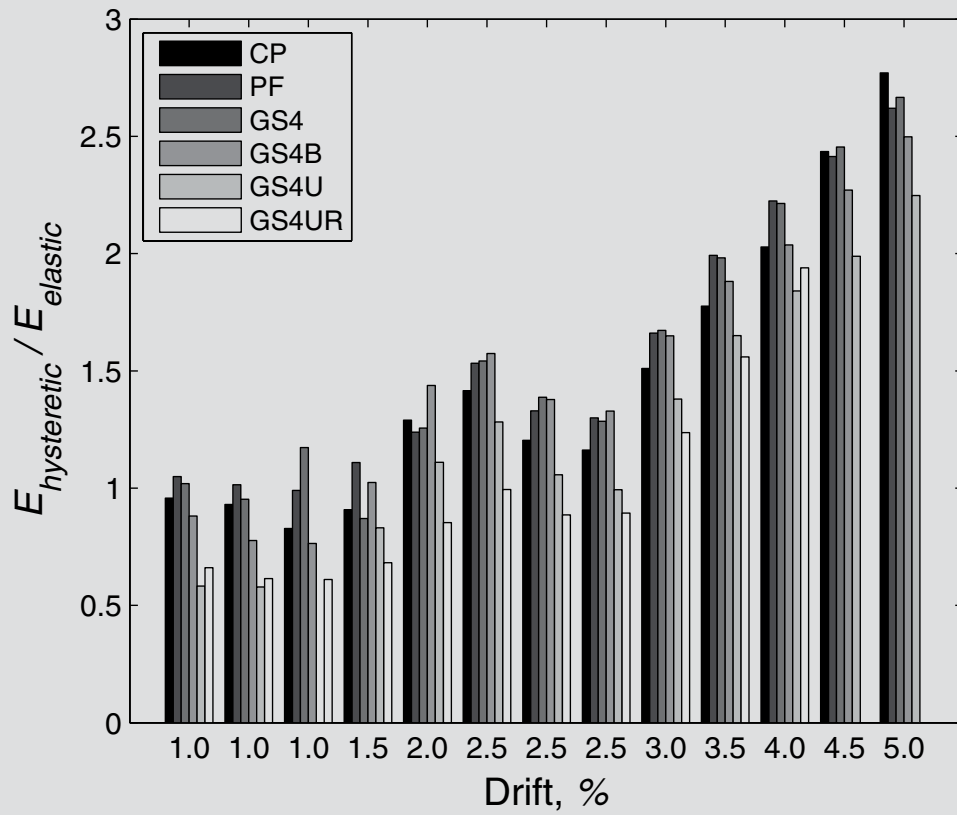


Figure 8. Dimensionless energy of the column-to-foundation connections. Note: $E_{elastic}$ = elastic energy; $E_{hysteretic}$ = hysteretic energy.

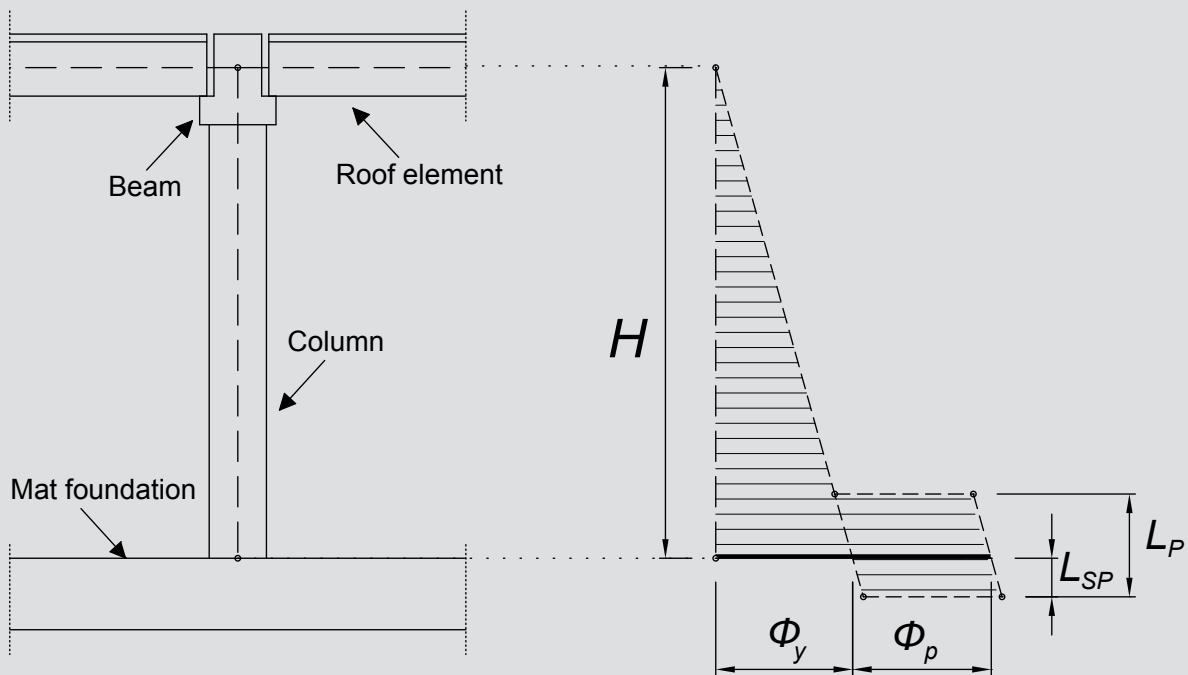


Figure 9. Column-curvature idealization. Note: H = column height; L_p = plastic hinge length; L_{sp} = strain penetration length; ϕ_p = column plastic curvature; ϕ_y = column yield curvature.

$$\Delta_y = \frac{\phi_y H^2}{3} + \phi_y L_{umb} H \quad (2)$$

where

ϕ_y = column yield curvature

$$\Delta_u = \Delta_y + \Delta_p \quad (3)$$

where

Δ_p = column displacement associated with plastic hinge rotation

$$= (\phi_u - \phi_y) L_p H \quad (4)$$

where

ϕ_u = column ultimate curvature

Equations (2) to (4) were applied to find the yield and ultimate drift associated with specimens GS4B and GS4U, that is, the grouted steel sleeve connection with and without the unbonded region. **Figure 10** shows the performance enhancement in terms of displacement capacity increase. The adoption of an unbonded length of reinforcement leads to a reduction of the curvature demand at a given imposed lateral displacement and therefore to a reduction of the column damage that is directly related to the curvature demand.

In the case of debonding, the ultimate reinforcing bar capacity is ensured, providing an appropriate development length in addition to the unbonded length. The use of grouted steel sleeves contributes to reducing the development length due to the sleeves' ability to restrain the splitting cracks in the grout rather than providing passive confinement. Although the aim of the research is not the determination of the bond strength associated with grouted steel sleeves, the use of the sleeves, especially with debonding, resulted in significant column lateral displacement without reinforcement bar failure.

Conclusion

The experimental program showed that grouted steel sleeves are suitable as column-to-foundation connections in seismic regions. The high ductility of the grouted steel sleeve connections is related to the confining effect of the corrugated steel sleeves on the grout. Furthermore, the presence of a highly confined grout prevents buckling of the longitudinal reinforcement.

In such connections, the damage was localized to the 20 mm (0.8 in.) grout layer between the precast concrete column and the foundation. As a result, little damage oc-

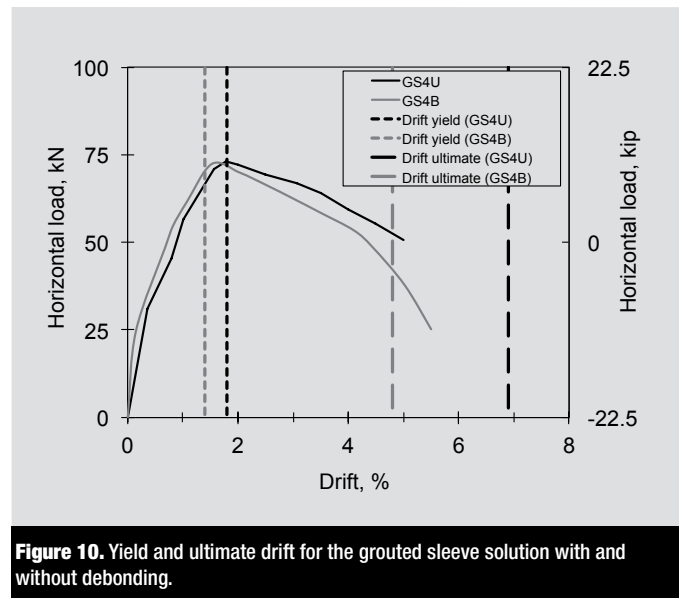


Figure 10. Yield and ultimate drift for the grouted sleeve solution with and without debonding.

curs in the column outside the base section. Due to the damage localization observed, the postseismic column repair for the grouted sleeve connection is simpler than that for cast-in-place concrete or pocket foundation connections and can be effectively done by replacing the base layer of crushed grout with new high-strength grout. To further reduce the column damage and increase the column lateral displacement capacity, an unbonded length of steel reinforcement can be used within the grouted sleeves. The proposed equations make it possible to take into account the unbonded length of reinforcement in the design process and to evaluate the column yield and ultimate displacement when unbonded reinforcing bars are used.

Acknowledgments

The experimental program reported in this paper was part of a research program on precast concrete column-to-foundation connections financed by Moretti SpA in Erbusco, Italy.

The cooperation of Cristian Ratti, Andrea Zini, and Nicola Barzi in setting up the reaction frame and conducting the experimental tests is acknowledged.

References

1. *fib* (International Federation for Structural Concrete) Commission 7. 2003. *Seismic Design of Precast Concrete Building Structures*, *International Federation for Structural Concrete*. Bulletin 27. Lausanne, Switzerland: *fib*.
2. PCI Connection Details Committee. 2008. *PCI Connections Manual for Precast and Prestressed Concrete Construction*. 1st ed. Chicago, IL: PCI.

3. Elliott, K. S. 2005. *Precast Concrete Structures*. Oxford, Great Britain: Elsevier Butterworth-Heinemann.
4. Blandón, J. J., and M. E. Rodríguez. 2005. Behavior of Connections and Floor Diaphragms in Seismic-Resisting Precast Concrete Buildings. *PCI Journal*, V. 50, No. 2 (March–April): pp. 56–75.
5. Martins, R., F. Canha, M. K. El Debs, K. de Borja Jaguaribe Jr., and A. L. Homce de Cresce El Debs. 2009. Behavior of Socket Base Connections Emphasizing Pedestal Walls. *ACI Structural Journal*, V. 106, No. 3 (May–June): pp. 268–278.
6. Osanai, Y., F. Watanabe, and S. Okamoto. 1996. Stress Transfer Mechanism of Socket Base Connections with Precast Concrete Columns. *ACI Structural Journal*, V. 93, No. 3 (May–June): pp. 1–11.
7. Priestley, M. J. N. 2002. Direct Displacement-Based Design of Precast/Prestressed Concrete Buildings. *PCI Journal*, V. 47, No. 6 (November–December): pp. 66–79.
8. Priestley, M. J. N., and D. N. Grant. 2005. Viscous Damping, in Seismic Design and Analysis. *Journal of Earthquake Engineering*, V. 9, Special Issue 2: pp. 229–255.
9. Priestley, M. J. N., G. M. Calvi, and M. J. Kowalsky. 2007. *Displacement-Based Seismic Design of Structures*. Pavia, Italy: IUSS Press.

- P = axial load
- $P-\Delta$ = 2nd order load-displacement effects
- Δ_p = column displacement associated with plastic hinge rotation
- Δ_u = column ultimate displacement
- Δ_y = column yield displacement
- μ_ϕ = curvature ductility
- ϕ = column curvature
- ϕ_p = column plastic curvature
- ϕ_y = column yield curvature
- ϕ_u = column ultimate curvature

Notation

- B = column cross-section height
- d_b = reinforcing bar diameter
- $E_{elastic}$ = elastic energy
- $E_{hysteretic}$ = hysteretic energy
- f_u = steel ultimate stress
- f_y = steel yield stress
- H = column height
- L_c = column contraflexure length
- L_p = plastic hinge length
- L_{sp} = strain penetration length
- L_{unb} = unbonded length

About the authors



Andrea Belleri, PhD, is a post-graduate fellow at the Department of Design and Technologies at the University of Bergamo in Bergamo, Italy.



Paolo Riva, PhD, is a full professor in the Department of Design and Technologies at the University of Bergamo.

Abstract

The paper investigates the suitability of grouted sleeve connections as column-to-foundation connections for precast concrete structures in seismic regions. Although grouted sleeves are commonly used, the typical advantages from this connection have not been fully addressed in the literature.

Experiments on the cyclic behavior of column-to-foundation subassemblies compared the response of grouted sleeve connections with cast-in-place and pocket-foundation connections.

The results demonstrate that grouted sleeves ensure a ductility and energy dissipation capacity similar to those of traditional connections. The confinement provided by the grouted sleeves inhibits buckling of the longitudinal reinforcement and increases the compressive strength of the grout. As a consequence, the damage associated with this kind of connection is localized to the column base, allowing easier postseismic column repair compared with traditional connections. The comparison of the experimental response of a grouted sleeve connection with partly unbonded reinforcement within the sleeves and the same specimens after retrofitting is also included.

Keywords

Connection, debonding, grouted sleeve, pocket foundation, seismic retrofit.

Review policy

This paper was reviewed in accordance with the Precast/Prestressed Concrete Institute's peer-review process.

Reader comments

Please address any reader comments to journal@pci.org or Precast/Prestressed Concrete Institute, c/o *PCI Journal*, 200 W. Adams St., Suite 2100, Chicago, IL 60606. ¶